

# Xanthohumol induces apoptosis and S phase cell cycle arrest in A549 non-small cell lung cancer cells

Wai Kuan Yong, Yen Fong Ho, Sri Nurestri Abd Malek

Institute of Biological Sciences, Faculty of Science, University of Malaya, Kuala Lumpur, Malaysia

Submitted: 12-12-2014

Revised: 02-02-2015

Published: 24-09-2015

## ABSTRACT

**Background:** Xanthohumol, a major prenylated chalcone found in female hop plant, *Humulus lupulus*, was reported to have various chemopreventive and anti-cancer properties. However, its apoptotic effect on human alveolar adenocarcinoma cell line (A549) of non-small cell lung cancer (NSCLC) was unknown. **Objective:** This study aimed to investigate the effects of xanthohumol on apoptosis in A549 human NSCLC cells. **Materials and Methods:** A549 cell proliferation was determined by sulforhodamine B assay. Morphological changes of the cells were studied via phase contrast and fluorescent microscopy. Induction of apoptosis was assessed by Annexin-V fluorescein isothiocyanate/propidium iodide (Annexin V-FITC/PI) staining, DNA fragmentation (TUNEL) assay mitochondrial membrane potential assay, cell cycle analysis, and caspase activity studies. **Results:** Xanthohumol was found to decrease cell proliferation in A549 cells but had relatively low cytotoxicity on normal human lung fibroblast cell line (MRC-5). Typical cellular and nuclear apoptotic features were also observed in A549 cells treated with xanthohumol. Onset of apoptosis in A549 cells was further confirmed by externalization of phosphatidylserine, changes in mitochondrial membrane potential, and DNA fragmentation in the cells after treatment. Xanthohumol induced accumulation of cells in sub G1 and S phase based on cell cycle analysis and also increased the activities of caspase-3, -8, and -9. **Conclusion:** This work suggests that xanthohumol as an apoptosis inducer, may be a potent therapeutic compound for NSCLC.

**Key words:** Human alveolar adenocarcinoma cell line, apoptosis, cell cycle, lung cancer, xanthohumol

## INTRODUCTION

Lung cancer is the leading cause of death among various types of cancers, and accounts for 1.38 million deaths worldwide, as of 2008.<sup>[1]</sup> There are two main types of lung cancer: small cell lung cancer (SCLC) which comprises 15–20% of total lung cancer cases, and non-small cell lung cancer (NSCLC) which comprises 80–85% of all lung cancer cases. The 5 years survival rate for NSCLC is <15% and even lower in SCLC.<sup>[2]</sup> Besides surgery, radiation therapy, and chemotherapy, targeted therapies are currently used to treat lung cancer for their specificity in reducing side effects of conventional treatments. Some examples of drugs currently used in targeted therapies for lung cancer are erlotinib, bevacizumab, and crizotinib.

Ongoing research efforts are carried out to discover new agents for both types of lung cancer to achieve a better favorable efficacy-to-toxicity profile.<sup>[3]</sup>

Xanthohumol (2', 4, 4'-trihydroxy-3'-prenyl-6'-methoxychalcone) [Figure 1] is a natural compound of the female hop plant, *Humulus lupulus*, and is the major prenylated chalcone of the plant. It was known as a “broad spectrum” chemopreventive agent for its ability to inhibit initiation (metabolic activation of procarcinogens), promotion (activation of carcinogen-detoxifying enzymes), and progression of tumor development.<sup>[4]</sup> Xanthohumol was reported to induce apoptosis in cancer cell lines such as prostate cancer cells,<sup>[5]</sup> hepatocellular carcinoma,<sup>[6]</sup> ovarian cells,<sup>[7]</sup> and malignant glioblastoma cells.<sup>[8]</sup> Previous studies showed that xanthohumol targets all three apoptotic pathways: the extrinsic (death receptor-mediated) pathway, intrinsic (mitochondria-mediated) pathway, and the endoplasmic reticulum stress and unfolded protein response pathway.<sup>[9]</sup>

### Address for correspondence:

Prof. Sri Nurestri Abd Malek, Institute of Biological Sciences,  
Faculty of Science, University of Malaya,  
50603 Kuala Lumpur, Malaysia.  
E-mail: srimalek@um.edu.my

### Access this article online

#### Website:

www.phcog.com

#### DOI:

10.4103/0973-1296.166069

#### Quick Response Code:



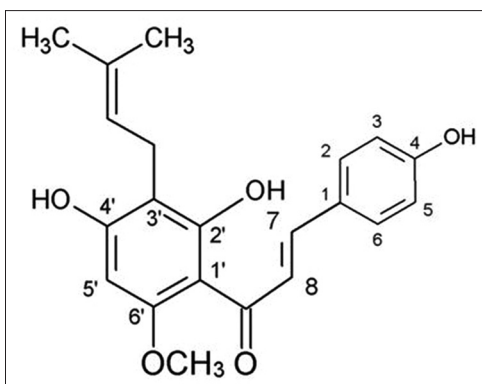


**Figure 1:** Xanthohumol

Xanthohumol was reported to induce cytotoxicity against human alveolar adenocarcinoma cell line (A549) cells via the inhibition of DNA topoisomerase I (Top 1) activity.<sup>[10]</sup> Top 1 is involved in the relaxation of supercoiled DNA during replication and transcription. Top 1 exists in higher level in tumor cells than normal body cells and hence has become a target for chemotherapeutic drugs such as camptothecin and etoposide. These drugs, known as Top 1 inhibitors or Top 1 poisons, inhibit the activities of Top 1 by preventing DNA religation step. This leads to DNA lesions and the initiation of cell cycle arrest, DNA repair and/or apoptosis.<sup>[11]</sup> Review articles also discussed the great potential of Top 1 inhibitors to be used together in radiotherapy as a combination therapy for lung cancer.<sup>[12,13]</sup> However, no further study was reported on the anti-cancer properties and the apoptotic-inducing effects of xanthohumol on lung cancer cells. Hence, in this study, we aimed to further investigate the anti-cancer properties of xanthohumol on A549 lung cancer cells by studying its role on cell proliferation, induction of apoptosis, cell cycle arrest, and caspase activities.

## MATERIALS AND METHODS

### Chemicals and materials

Xanthohumol was purchased from Biobiopha Co., Ltd., China. Doxorubicin hydrochloride, dimethyl sulfoxide (DMSO), sulforhodamine B (SRB), Hoechst 33342, and propidium iodide (PI) were purchased from Sigma, USA. Roswell Park Memorial Institute (RPMI) 1640 medium, fetal bovine serum (FBS), penicillin/streptomycin, and amphotericin B were obtained from PAA Laboratories, Austria. Xanthohumol was dissolved in DMSO and diluted to various concentrations with 10% fetal bovine serum- (FBS-) supplemented media, achieving the final concentration of 0.5%DMSO. Fluorescein isothiocyanate (FITC) annexin V apoptosis detection kit, mitochondrial membrane detection kit, and caspase-3 assay

kit were supplied by BD Biosciences, USA. APO-BrdU terminal deoxynucleotidyl transferase dUTP nick end labeling (TUNEL) assay kit was purchased from Molecular Probes, USA. Caspase-8 and caspase-9 activity kits were purchased from Promega, USA.

### Cell culture

Human alveolar adenocarcinoma cell line (A549) and human fetal lung fibroblast cell line (MRC-5) cell lines were obtained from American Type Culture Collection, USA. A549 cells were cultured in RPMI 1640 medium containing 10% FBS, 2% penicillin/streptomycin, and 1% amphotericin B. MRC-5 cells were cultured in Minimum Essential Medium (MEM) supplemented with 10% FBS and 1% penicillin/streptomycin. Cells were maintained at 37°C with 5% CO<sub>2</sub> saturation.

### Sulforhodamine B assay

This assay method is adapted from Houghton.<sup>[14]</sup> 8,000 cells/well were seeded into a 96-well plate and incubated overnight for adherence. At the end of incubation, media in each well was discarded and replaced by various concentrations of xanthohumol or doxorubicin for 24, 48, and 72 h treatment periods. Treatment periods were ended by adding 50 µl of 40% cold trichloroacetic acid (TCA) acid (w/v) to each well. The plates were incubated for 1 h at 4°C before supernatant were discarded. Each well was then washed with 50 µl of distilled water for 5 times and air-dried. 50 µl of SRB (0.4% w/v in 1% acetic acid) was added to each well and incubated for 30 min at room temperature for the staining process. To remove unbound dye, each well was washed with 50 µl of 1% acetic acid for 5 times and air-dried. 100 µl Tris base (10 mM unbuffered, pH 10.5) was added to each well. To solubilize bound SRB dyes, the plate was shaken at 500 rpm for 5 min. Absorbance values were measured at 492 nm using Synergy H1 Hybrid. IC<sub>50</sub> values were determined by plotting dose response curves using percentage of inhibition of cell proliferation against treatment concentrations.

### Phase contrast microscopy

A549 cells seeded in 24-well plates (5 × 10<sup>4</sup> cells/well) were treated with 14, 28, and 42 µM xanthohumol for 72 h. Cells were then observed under AxioCam ERC5s inverted phase contrast microscope.

### Hoechst/propidium iodide staining

1.0 × 10<sup>6</sup> cells were seeded in each 6 cm culture dish and allowed to adhere overnight. The cells were treated with various concentrations of xanthohumol for 72 h. At the end of incubation period, the media in the culture dishes were discarded and were washed

with cold phosphate-buffered saline (PBS). 1 ml of cold PBS was added to each culture dish. To stain the cells with fluorescent dyes, 100  $\mu\text{L}$  of Hoechst solution (100  $\mu\text{g}/\text{ml}$ ) and 25  $\mu\text{L}$  PI solution (100  $\mu\text{g}/\text{ml}$ ) were added to each culture dish and incubated for 15 min. The cells were observed under Leica DMI6000B fluorescent microscope.

#### Apoptosis detection by annexin V-fluorescein isothiocyanate/propidium iodide (annexin V-FITC/PI) staining

FITC annexin V Apoptosis Detection Kit was used to detect apoptosis. Cells were seeded in 6-well plates ( $2.4 \times 10^5$  cells/well) and allowed to adhere overnight. Then, the cells were treated with 14, 28, and 42  $\mu\text{M}$  of xanthohumol for 72 h. The cells were harvested, washed and resuspended in  $1 \times$  binding buffer.  $1 \times 10^5$  cells were stained with 5  $\mu\text{L}$  of FITC-Annexin V and 5  $\mu\text{L}$  of PI. Unstained and single stained untreated cells were also included as controls. 10,000 were acquired for each replicate using Accuri C6 flow cytometer.

#### Mitochondrial membrane potential assay

JC-1, a lipophilic and cell-permeable fluorochrome was used to measure the changes in mitochondrial membrane potential ( $\Delta\Psi_m$ ), according to the manufacturer's instruction. Cells seeded in six-well plates were treated with 14, 28, and 42  $\mu\text{M}$  of xanthohumol for 72 h. After treatment, cells were harvested and incubated with JC-1 working solution for 15 min. The cells were washed and resuspended in  $1 \times$  assay buffer. The intracellular fluorescence (FL) signal intensity of JC-1 was measured by Accuri C6 flow cytometer.

#### DNA fragmentation by transferase dUTP nick end labeling assay

DNA strand breaks in apoptotic cells were detected by APO-BrdU TUNEL assay kit. After incubation with xanthohumol at 14, 28, and 42  $\mu\text{M}$  for 72 h, cells were harvested and washed with PBS. Then, the cells were fixed with 1% (w/v) paraformaldehyde for 15 min, washed with PBS, and fixed with 70% (v/v) ethanol overnight. Ethanol was removed by centrifugation and DNA labeling steps were performed according to manufacturer's instructions. Samples were analyzed by flow cytometer and 10,000 events were acquired for each replicate.

#### Cell cycle analysis

At 72 h after treatment with xanthohumol, adherent and floating cells were collected, centrifuged, and fixed in 70% ethanol overnight. Samples were centrifuged and washed with cold PBS. The cells were then resuspended in 300  $\mu\text{L}$  of staining solution containing final concentrations of 50  $\mu\text{g}/\text{ml}$  PI, 50  $\mu\text{g}/\text{ml}$  RNase, 0.1% triton X-100, 1 mg/ml sodium citrate, and distilled water.<sup>[15]</sup> After 30 min

incubation at room temperature, cells were analyzed using flow cytometer and data analysis was performed by Modfit LT software, USA.

#### Caspase-3 activity

Caspase-3 activity assay was carried out according to manufacturer's instruction. Briefly, cells seeded in 6-well plates at a density of  $3.0 \times 10^5$  cells/well were treated with various concentrations of xanthohumol and different incubation time (12, 24, and 48 h). At the end of treatment, cells were harvested, washed with PBS, and lysed in the cold lysis buffer for 30 min on ice. In a 96-well plate, 200  $\mu\text{L}$  of HEPES buffer, 5  $\mu\text{L}$  acetyl Asp-Glu-Val-Asp 7-amido-4-methylcoumarin (Ac-DEVD-AMC) substrate, and 50  $\mu\text{L}$  cell lysate were added to each well. The reaction mixtures were incubated for 1 h at 37°C. AMC liberated was measured using Synergy H1 Hybrid with 380 nm as excitation wavelength and 440 nm as emission wavelength.

#### Caspase-8 and caspase-9 activity

Caspase-8 and caspase-9 activity assays were performed according to manufacturer's instruction. Cells were seeded at a density of 25,000 cells/well in white-walled 96 well plates. After treatment with different doses of xanthohumol and incubation period of 12, 24, and 48 h, the plates were equilibrated to room temperature and then 100  $\mu\text{L}$  Caspase-Glo<sup>®</sup> Reagent were added to each well. After incubation for 1 h, luminescence of each test sample was measured by Synergy H1 Hybrid.

#### Statistical analysis

Values are shown as mean  $\pm$  standard error of the mean. Experiments were done at least twice with triplicates. Flow cytometry plots are representative of the experiment replicates. Comparison between control and treated groups was made using one-way analysis of variance with *post-hoc* Tukey test.  $P < 0.05$  was considered statistically significant. All calculations were performed using SPSS version 17.0, USA.

## RESULTS

#### Xanthohumol decreases cell viability and proliferation of A549 cells

The results from SRB assay showed that xanthohumol inhibited cell proliferation and viability in dose- and time-dependent manner [Figure 2a]. The  $\text{IC}_{50}$  values of XN on A549 cells were  $74.06 \pm 1.98 \mu\text{M}$ ,  $25.48 \pm 0.30 \mu\text{M}$ , and  $13.50 \pm 0.82 \mu\text{M}$  at 24, 48, and 72 h, respectively.

The  $\text{IC}_{50}$  values of xanthohumol on MRC-5 were much higher than the  $\text{IC}_{50}$  values of xanthohumol on A549. This

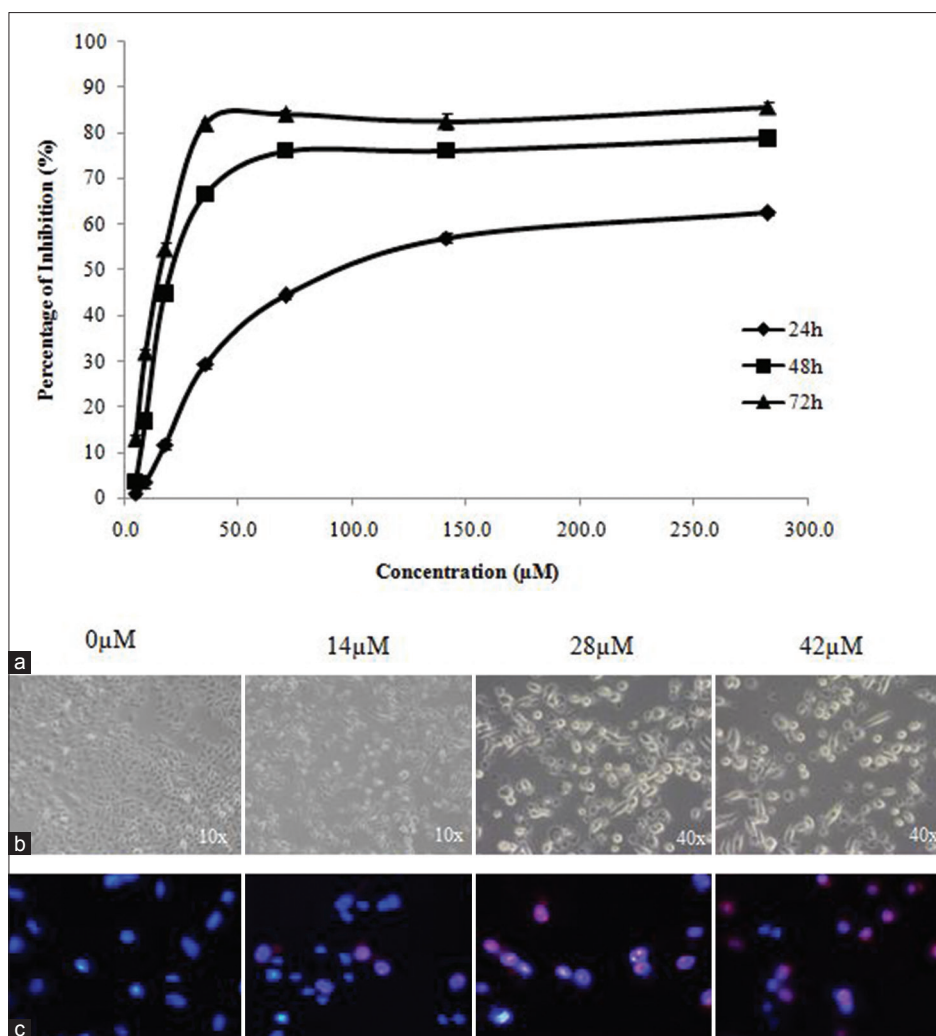


**Figure 2:** (a) The inhibition effects of xanthohumol on proliferation of A549 cells after 24, 48 and 72 h of treatment. Data are presented as the mean values  $\pm$  standard error of mean of triplicates. (b) Phase contrast microscopy for cells treated with various concentrations of xanthohumol at different magnification. (c) Hoechst/propidium iodide double staining showing nuclear morphological differences between untreated cells (0  $\mu$ M) and treated cells (14, 28, 42  $\mu$ M for 72 h) at 40x magnification

indicates that xanthohumol was less toxic to normal cells compared to cancer cells *in vitro*. Doxorubicin was used as a reference compound in both cell lines. The  $IC_{50}$  values were presented in Table 1.

### Xanthohumol induces typical apoptotic morphological changes

Under phase contrast microscopy [Figure 2b], untreated A549 cells were adherent, elongated in shape, high confluency and closely arranged. Xanthohumol-treated cells displayed atrophy, size shrinkage, decrease in cell number, and detachment of cells. These are characteristic features of cells undergoing apoptosis.<sup>[16]</sup>

To observe changes in cell nucleus upon treatment, cells were stained with Hoechst 33342 and PI nuclear dyes. Untreated A549 cells had dim nuclei that were uniformly stained by Hoechst stain [Figure 2c]. After treatment,

the DNA of the apoptotic cell nucleus was observed to be brighter, fragmented, and condensed. At higher concentrations, increased number of late apoptotic/necrotic cells (stained red by PI due to permeabilized membrane) were observed.

### Xanthohumol induces externalization of phosphatidylserine and loss of mitochondrial membrane potential ( $\Delta \psi$ m)

Apoptosis induced by xanthohumol on A549 was confirmed using Annexin V-FITC/PI assay. Figure 3a shows that cells treated with higher concentration of xanthohumol showed higher percentage of cells at early apoptosis (Annexin V-FITC<sup>+</sup>PI<sup>-</sup>, lower right quadrant) and late apoptosis or secondary necrosis (Annexin V-FITC<sup>+</sup>PI<sup>+</sup>, upper right quadrant). The percentage of early apoptotic cells increased significantly from  $1.42 \pm 0.47\%$  (negative control, 0  $\mu$ M) to  $2.72 \pm 0.59\%$ ,

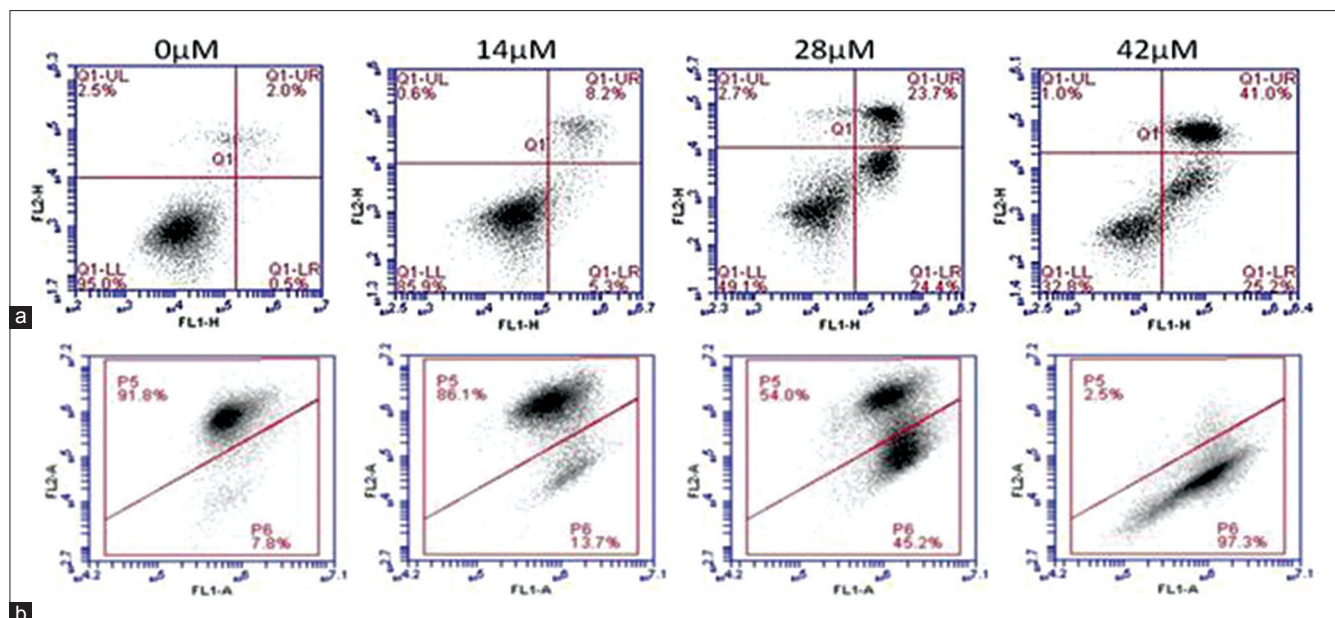


**Figure 3:** (a) Xanthohumol induces early and late apoptosis. From the flow cytometry analysis, the first quadrant (lower left) depicts percentage of viable cells, second quadrant (lower right) depicts percentage of early apoptotic cells, third quadrant (upper right) depicts late apoptotic or secondary necrotic cells and fourth quadrant (upper left) depicts primary necrotic cells. (b) Xanthohumol treatment results in a shift in mitochondrial membrane potential. Viable cells with active mitochondria have high  $\Psi_m$  and form JC-1 aggregates (P5 region). Mitochondria of apoptotic or necrotic cells have low  $\Psi_m$  and JC-1 remains as monomer (P6 region)

**Table 1: IC<sub>50</sub> values (μM) of xanthohumol and doxorubicin on A549 human lung cancer cell line and MRC-5 human lung fibroblast at 24, 48, and 72 h of treatment determined using SRB assay**

Cell line	Growth inhibition, IC <sub>50</sub> (μM)					
	Xanthohumol			Doxorubicin		
	24 h	48 h	72 h	24 h	48 h	72 h
A549	74.06±1.98	25.48±0.30	13.50±0.82	2.85±0.20	0.22±0.03	0.02±0.02
MRC-5	>282 (>100ug/mL)	149.20±4.96	94.38±1.77	5.71±0.55	2.01±0.04	1.09±0.10

Tabulated values are mean±SEM. SEM: Standard error of mean; MRC-5: Human fetal lung fibroblast cell line; A549: Human alveolar adenocarcinoma cell line; SRB assay: Sulforhodamine B colorimetric assay

26.08 ± 1.50%, and 34.42 ± 4.41% upon treatment with 14, 28, and 42 μM of xanthohumol, respectively. Population of late apoptotic or secondary necrotic cells also increased significantly from 1.80 ± 0.30% (negative control) to 4.90 ± 0.85%, 17.05 ± 3.12%, and 33.27 ± 3.55%, respectively.

As shown in Figure 3b,  $\Delta \Psi_m$  of A549 cells was significantly reduced by xanthohumol in a dose-dependent manner. The percentage of cells in P6 region indicates apoptotic cell population with a reduction in  $\Delta \Psi_m$ . Population of viable cells (P5 region) reduced significantly from 91.42 ± 0.36% for untreated sample to only 2.88 ± 0.62% at 42 μM xanthohumol treatment. In viable cells with high  $\Delta \Psi_m$ , JC-1 monomers combine and form aggregates with intense red FL, which can be detected in FL2-A channel. In apoptotic cells with reduced or depolarized  $\Delta \Psi_m$ , JC-1 molecules remain as J-monomers with intense green FL detected in FL1-A channel.<sup>[17]</sup>

### Xanthohumol induces DNA fragmentation and cell cycle arrest at S phase

TUNEL (Terminal deoxynucleotidyl transferase-mediated dUTP nick end labelling) assay was used to detect DNA fragmentation and identify individual cells that were undergoing apoptosis.<sup>[17]</sup> Figure 4a and b shows that percentage of cells with DNA fragmentation increased significantly in comparison to the negative control (4.27 ± 0.13%) to 34.7 ± 0.30% and 39.2 ± 0.15% for A549 cells treated with 28 μM and 42 μM xanthohumol, respectively.

The effect of xanthohumol on cell cycle progression was analyzed using PI staining. Increasing concentration of xanthohumol increased the percentage of cells arrested at sub G1 peak, an observation corresponding to apoptotic cells with sub-diploid DNA<sup>[17]</sup> [Figure 4c and d]. Furthermore, there is significant accumulation of cells at S phase with the percentage of cells increased from

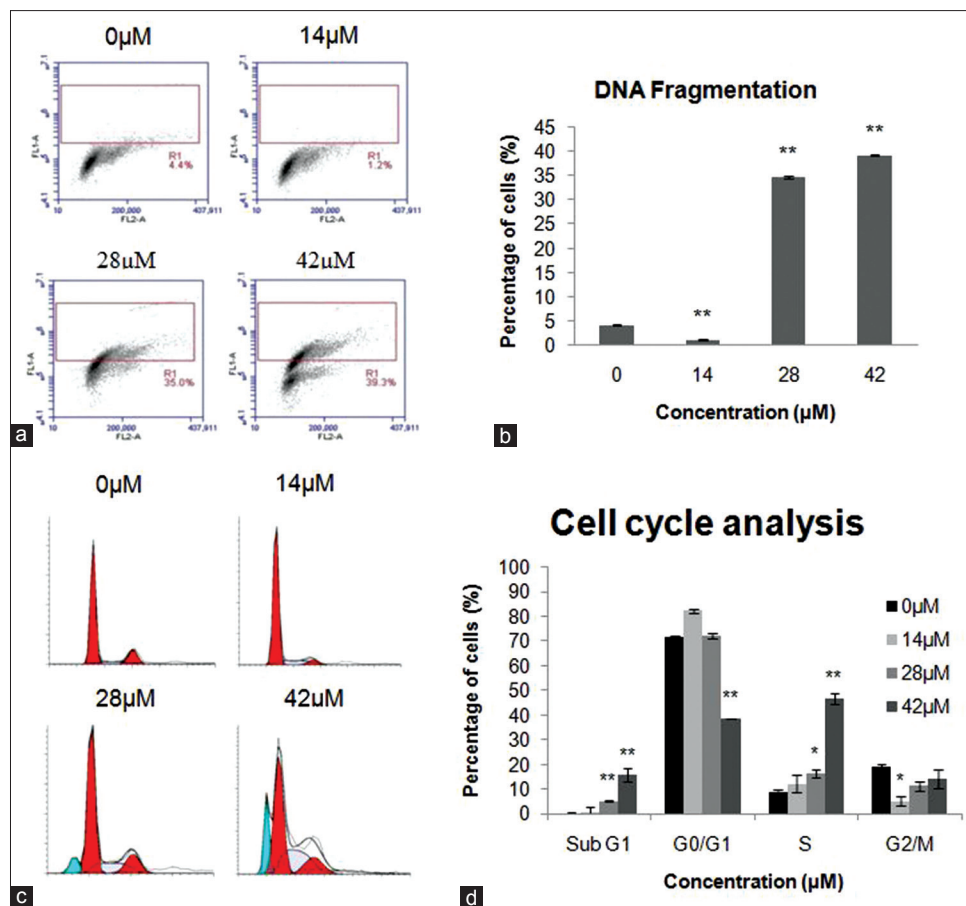


**Figure 4:** (a) Xanthohumol induces DNA fragmentation. Percentage of cells in R1 region represents cells with DNA fragmentation. (b) Statistical significance to control is marked with \*\* ( $P < 0.01$ ). (c) Cell cycle progression. The percentage of apoptotic cells at hypodiploid DNA peak (sub-G1 population, blue peak) and percentage of cells accumulated at S phase increased at higher concentrations. (d) Percentage of cells at various cell cycle phases. Statistical significance to control is marked with (\*) ( $P < 0.05$ ) and (\*\*) ( $P < 0.01$ )

$8.94 \pm 0.23\%$ ,  $12.34 \pm 1.09\%$ , and  $16.43 \pm 1.52\%$  to  $46.95 \pm 2.03\%$  at 0, 14, 28, and 42  $\mu\text{M}$  xanthohumol, respectively.

#### Activation of caspase-3, -8 and -9 in xanthohumol-induced apoptosis

As shown in Figure 5, exposure of A549 to xanthohumol led to increase in caspase-3, -8, and -9 activities. Caspase-3 activity was measured by the release of fluorescent AMC upon cleavage of fluorogenic substrate Ac-DEVD-AMC. The results showed that the RFU values increased as concentration and treatment time increased. This indicated more caspase-3 enzymes were activated. Caspase-8 and -9 activities were measured upon cleavage of luminogenic substrates, releasing aminoluciferin which reacted with luciferase and emitted luminescence signals. For both caspase-8 and -9 activities, the highest RLU values were observed for cells treated with 14  $\mu\text{M}$  xanthohumol at 24 h and 48 h. Xanthohumol treatment significantly increased the activities of caspase-8 and -9.

## DISCUSSION

Xanthohumol was reported to be an effective agent to induce cell death in different cancer cell lines such as liver, breast, prostate, endometrial colon cancer, as well as leukemia, myeloma, sarcoma and melanoma cell lines, macrophages, adipocytes, dendritic cells, and *t*-cells. Biochemical effects were induced by xanthohumol at concentrations ranging from 0.1–100  $\mu\text{M}$  depending on cell lines and treatment periods.<sup>[9]</sup> This study aimed to provide further information on the application of xanthohumol in lung cancer treatment.

Our results demonstrated that xanthohumol decreased cell viability and proliferation of A549 cells. Morphological studies revealed typical cell death characteristics such as size shrinkage, reduction in cell number, detachment of cells, formation of apoptotic bodies, nuclear fragmentation, and permeabilized cell membrane. Onset of apoptosis such as externalization of phosphatidylserine, changes in mitochondrial membrane potential, and DNA

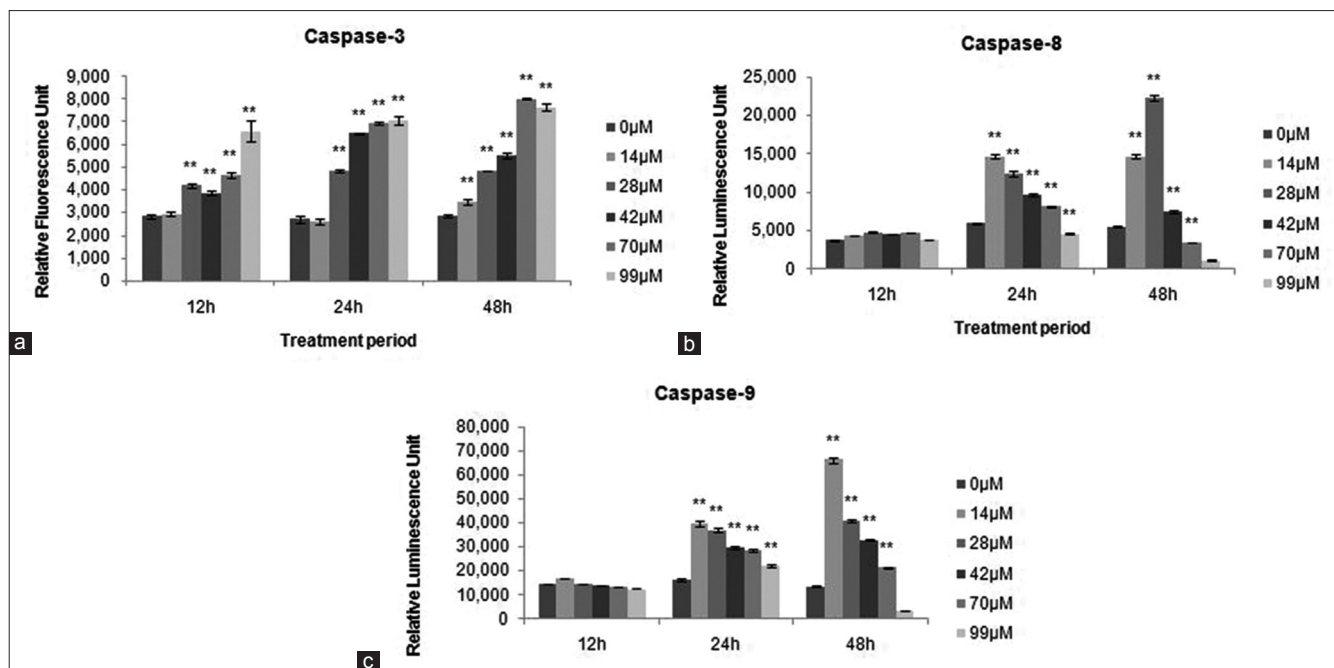


**Figure 5:** Xanthohumol increased activity of (a) caspase-3, (b) caspase-8, and (c) caspase-9 activity at 12, 24, and 48 h. Statistical significance to control is marked with (\*) ( $P < 0.05$ ) and (\*\*) ( $P < 0.01$ )

fragmentation were also observed in cells after treatment. Cell cycle analysis revealed that xanthohumol-induced S-phase arrest and the compound also increased the activity of caspase-3, -8, and -9. S phase is defined as the time during the cell cycle when DNA synthesis is taking place, leading to a doubling amount of DNA per cell.

The cytotoxic effects of xanthohumol on A549 cells had been previously reported by Lee *et al.*,<sup>[10]</sup> with the  $IC_{50}$  values of  $4.3 \mu\text{g/ml}$  (approximately  $12.14 \mu\text{M}$ ) for xanthohumol and  $0.5 \mu\text{g/ml}$  (approximately  $0.86 \mu\text{M}$ ) for doxorubicin after 48 h treatment. However, in our study, the  $IC_{50}$  values after 48 h were  $25.48 \mu\text{M}$  for xanthohumol and  $0.22 \mu\text{M}$  for doxorubicin. Our findings are approximately two times higher for xanthohumol and three times lower for doxorubicin than the values reported by Lee *et al.*, interestingly, our  $IC_{50}$  value for 72 h treatment period ( $13.50 \mu\text{M}$ ) is more similar to the value reported by Lee *et al.*, at 48 h treatment period. Pinmai *et al.*,<sup>[18]</sup> also performed SRB assay on A549 cells using doxorubicin as a positive control and reported the  $IC_{50}$  value for doxorubicin as  $0.17 \pm 0.006 \mu\text{g/ml}$ , approximately  $0.0293 \mu\text{M}$ . This value is close to our finding, which is  $0.02 \mu\text{M}$  at 72 h. The differences in  $IC_{50}$  values between different reports might be due to different protocols, cell condition, and doubling time. Moreover, in our study, majority of xanthohumol-induced effects in A549 cells occurred significantly at 72 h treatment period. Hence, we are convinced that the concentrations and time selected in this study have effective cytotoxicity on the cells.

Xanthohumol was reported to induce cytotoxicity against A549 cells via the inhibition of DNA (Top 1) activity by Lee *et al.* Top 1 plays an important role in DNA replication and transcription by inducing single-strand breaks at the DNA to assist in the rotation of the DNA double helix. Intermediates called Top 1 cleavage complexes (Top 1 cc) are formed rapidly before Top 1 religates the strand breaks and regenerates intact duplex DNA. Top 1 exists in higher level in tumor cells than normal body cells. Hence, Top 1 inhibition has become a target in the treatment of NSCLC,<sup>[12]</sup> to induce DNA lesions and the initiation of cell cycle arrest, DNA repair and/or apoptosis.<sup>[11]</sup> In the present study, xanthohumol was shown to induce significant DNA fragmentation in A549 cells. Top 1 inhibitors such as camptothecin and etoposide are also reported to cause mitochondrial lesions and initiate the production of reactive oxygen species (ROS). Xanthohumol treatments on human cancer cell lines were reported to increase the release of mitochondria-derived ROS and subsequently trigger apoptosis induction via the intrinsic pathway.<sup>[19]</sup> Thus, ROS production appears to contribute to the changes in mitochondrial membrane potential in A549 cells.

Overexpression of anti-apoptotic protein, Bcl-2 in cancer cells was reported to prevent the formation of Top 1 cc. Xanthohumol was reported to be able to decrease the expression of Bcl-2 and induce apoptosis via the intrinsic pathway.<sup>[9]</sup> Apoptotic cell death induced by xanthohumol involves different mechanisms: the extrinsic, intrinsic, and endoplasmic reticulum stress-induced pathway. Both

extrinsic and intrinsic pathways converge on a common mechanism activated by caspases. Activation of caspase-8 and -9 further confirm the onset of apoptosis. Caspase-8 is activated by the death receptor signaling whereas caspase-9 is activated by the mitochondria-mediated pathway. Caspase-8 and -9 activate caspase-3, which leads to phosphatidylserine translocation and DNA fragmentation by proteolytic cleavage. In our study, xanthohumol increased the expression of caspase-3, -8, and -9 in A549 cells, which might then lead to the observations of phosphatidylserine translocation and increased DNA fragmentation. Activation of all caspase-3, -8, and -9 by xanthohumol has also been reported on HCT-116 human colon cancer cells in which apoptosis occurred via both death receptor and mitochondrial-mediated pathways.<sup>[20]</sup> The activation of caspases leads to ROS production from the mitochondria, which subsequently generate Top 1 cc.

Top 1 inhibitors have also been correlated to S phase arrest in the cell cycle and reduced DNA synthesis by initiating DNA damage and causing replication fork arrest. DNA lesions activate Chk1 protein, which subsequently results in intra-S-phase checkpoint by halting the initiation of DNA replication and elongation.<sup>[21]</sup> Camptothecin and topotecan are examples of top 1 inhibitors that induced S phase-associated DNA strand breaks and reduced DNA synthesis in the cells.<sup>[22]</sup> Our finding revealed that xanthohumol, as an inhibitor of Top 1, induced S phase arrest in A549 cells. S phase arrest by xanthohumol was also reported on benign prostatic hyperplasia (BPH-1) epithelial cell line treated with 10  $\mu\text{M}$  and 20  $\mu\text{M}$  for 48 h<sup>[23]</sup> and MDA-MB-435 breast cancer cells treated with 5–50  $\mu\text{M}$  xanthohumol for 24 h.<sup>[4]</sup>

Xanthohumol might have selective toxicity to lung cancer cells and normal lung cancer cells based on our results in the SRB assay. The  $\text{IC}_{50}$  values of xanthohumol on MRC-5 normal lung fibroblasts were many folds higher than the  $\text{IC}_{50}$  values of xanthohumol on A549 cell line [Table 1]. This indicates that xanthohumol is less cytotoxic to normal cells in lower doses. Monteiro *et al.*,<sup>[24]</sup> reported the *in vivo* antitumor effects of xanthohumol by testing on breast cancer xenografts in nude mice. Tumors isolated from xanthohumol treated mice showed a decrease in tumor-surrounding inflammatory cells and a large central necrosis. Several *in vivo* studies confirmed that the oral administration of xanthohumol to mice was safe without affecting major organ functions and side effects. Vanhoecke *et al.*,<sup>[25]</sup> tested the influence of xanthohumol on the function and integrity of bone marrow, liver, exocrine pancreas, kidneys, muscles, and endocrine organs. The results showed that there was no difference

in hematological and biochemical blood analyses between mice treated with xanthohumol and control group. Xanthohumol also did not affect the metabolism of lipids, carbohydrates, protein, uric acid, and ion regulation. Another study by Dorn *et al.*,<sup>[6]</sup> reported that feeding xanthohumol to mice did not impair organ function and homeostasis and high dose oral administration of xanthohumol in mice was safe.

## CONCLUSION

Based on our findings and those of previous studies, it can be concluded that xanthohumol, as a Top 1 inhibitor, induces apoptosis and S phase cell cycle arrest in A549 cells. This work suggests that xanthohumol is a potential anti-cancer agent for the treatment of lung cancer.

## ACKNOWLEDGMENTS

The authors wish to acknowledge the Ministry of Higher Education of Malaysia and the University of Malaya for financial assistance received through the HIR MOHE F000002-21001 Grant and IPPP PV149/2012A Grant.

## REFERENCES

1. Ferlay J, Shin HR, Bray F, Forman D, Mathers C, Parkin DM. Estimates of worldwide burden of cancer in 2008: GLOBOCAN 2008. *Int J Cancer* 2010;127:2893-917.
2. Pore MM, Hiltermann TJ, Krzyt FA. Targeting apoptosis pathways in lung cancer. *Cancer Lett* 2013;332:359-68.
3. Larsen JE, Cascone T, Gerber DE, Heymach JV, Minna JD. Targeted therapies for lung cancer: Clinical experience and novel agents. *Cancer J* 2011;17:512-27.
4. Gerhauser C, Alt A, Heiss E, Gamal-Eldeen A, Klimo K, Knauff J, *et al.* Cancer chemopreventive activity of xanthohumol, a natural product derived from hop. *Mol Cancer Ther* 2002;1:959-69.
5. Deeb D, Gao X, Jiang H, Arbab AS, Dulchavsky SA, Gautam SC. Growth inhibitory and apoptosis-inducing effects of xanthohumol, a prenylated chalcone present in hops, in human prostate cancer cells. *Anticancer Res* 2010;30:3333-9.
6. Dorn C, Weiss TS, Heilmann J, Hellerbrand C. Xanthohumol, a prenylated chalcone derived from hops, inhibits proliferation, migration and interleukin-8 expression of hepatocellular carcinoma cells. *Int J Oncol* 2010;36:435-41.
7. Drenzek JG, Seiler NL, Jaskula-Sztul R, Rausch MM, Rose SL. Xanthohumol decreases Notch1 expression and cell growth by cell cycle arrest and induction of apoptosis in epithelial ovarian cancer cell lines. *Gynecol Oncol* 2011;122:396-401.
8. Festa M, Capasso A, D'Acunto CW, Masullo M, Rossi AG, Pizza C, *et al.* Xanthohumol induces apoptosis in human malignant glioblastoma cells by increasing reactive oxygen species and activating MAPK pathways. *J Nat Prod* 2011;74:2505-13.
9. Strathmann J, Gerhauser C. Anti-proliferative and apoptosis-inducing properties of xanthohumol, a prenylated chalcone from hops (*Humulus lupulus* L.). In: Diederich M, Noworyta K, editors. *Natural Compounds as Inducers of Cell Death*. Netherlands: Springer; 2012. p. 69-93.



10. Lee SH, Kim HJ, Lee JS, Lee IS, Kang BY. Inhibition of topoisomerase I activity and efflux drug transporters' expression by xanthohumol from hops. *Arch Pharm Res* 2007;30:1435-9.
11. Sordet O, Khan QA, Pommier Y. Apoptotic topoisomerase I-DNA complexes induced by oxygen radicals and mitochondrial dysfunction. *Cell Cycle* 2004;3:1095-7.
12. Chhatrivala H, Jafri N, Salgia R. A review of topoisomerase inhibition in lung cancer. *Cancer Biol Ther* 2006;5:1600-7.
13. Chen AY, Chen PM, Chen YJ. DNA topoisomerase I drugs and radiotherapy for lung cancer. *J Thorac Dis* 2012;4:390-7.
14. Houghton P, Fang R, Techatanawat I, Steventon G, Hylands PJ, Lee CC. The sulphorhodamine (SRB) assay and other approaches to testing plant extracts and derived compounds for activities related to reputed anticancer activity. *Methods* 2007;42:377-87.
15. Vanparys C, Maras M, Lenjou M, Robbens J, Van Bockstaele D, Blust R, *et al.* Flow cytometric cell cycle analysis allows for rapid screening of estrogenicity in MCF-7 breast cancer cells. *Toxicol In Vitro* 2006;20:1238-48.
16. Elmore S. Apoptosis: A review of programmed cell death. *Toxicol Pathol* 2007;35:495-516.
17. Vermes I, Haanen C, Reutelingsperger C. Flow cytometry of apoptotic cell death. *J Immunol Methods* 2000;243:167-90.
18. Pinmai K, Chunlaratthanabhorn S, Ngamkitidechakul C, Soonthornchareon N, Hahnvajanawong C. Synergistic growth inhibitory effects of *Phyllanthus emblica* and *Terminalia bellerica* extracts with conventional cytotoxic agents: Doxorubicin and cisplatin against human hepatocellular carcinoma and lung cancer cells. *World J Gastroenterol* 2008;14:1491-7.
19. Strathmann J, Klimo K, Sauer SW, Okun JG, Prehn JH, Gerhäuser C. Xanthohumol-induced transient superoxide anion radical formation triggers cancer cells into apoptosis via a mitochondria-mediated mechanism. *FASEB J* 2010;24:2938-50.
20. Pan L, Becker H, Gerhäuser C. Xanthohumol induces apoptosis in cultured 40-16 human colon cancer cells by activation of the death receptor- and mitochondrial pathway. *Mol Nutr Food Res* 2005;49:837-43.
21. Seiler JA, Conti C, Syed A, Aladjem MI, Pommier Y. The intra-S-phase checkpoint affects both DNA replication initiation and elongation: Single-cell and -DNA fiber analyses. *Mol Cell Biol* 2007;27:5806-18.
22. Cliby WA, Lewis KA, Lilly KK, Kaufmann SH. S phase and G2 arrests induced by topoisomerase I poisons are dependent on ATR kinase function. *J Biol Chem* 2002;277:1599-606.
23. Colgate EC, Miranda CL, Stevens JF, Bray TM, Ho E. Xanthohumol, a prenylflavonoid derived from hops induces apoptosis and inhibits NF-kappaB activation in prostate epithelial cells. *Cancer Lett* 2007;246:201-9.
24. Monteiro R, Calhau C, Silva AO, Pinheiro-Silva S, Guerreiro S, Gärtner F, *et al.* Xanthohumol inhibits inflammatory factor production and angiogenesis in breast cancer xenografts. *J Cell Biochem* 2008;104:1699-707.
25. Vanhoecke BW, Delporte F, Van Braeckel E, Heyerick A, Depypere HT, Nuytinck M, *et al.* A safety study of oral tangeretin and xanthohumol administration to laboratory mice. *In Vivo* 2005;19:103-7.

**Cite this article as:** Yong WK, Ho YF, Abd Malek SN. Xanthohumol induces apoptosis and S phase cell cycle arrest in A549 non-small cell lung cancer cells. *Phcog Mag* 2015;11:275-83.

**Source of Support:** Ministry of Higher Education of Malaysia through the HIR MOHE F000002-21001 Grant and the University Of Malaya through the IPPP PV149/2012A Grant. **Conflict of Interest:** None declared.